Received: 26 November 2023 | Revised: 9 April 2024 | Accepted: 18 April 2024

DOI: 10.1096/fj.202302423RR

RESEARCH ARTICLE

The FASEB Journal

Biosensor capability of the endometrium is mediated in part, by altered miRNA cargo from conceptus-derived extracellular vesicles

Tiago H. C. De Bem[1,2] | Alessandra Bridi[2] | Haidee Tinning[1] | Rafael Vilar Sampaio[2] | Irene Malo-Estepa[1] | Dapeng Wang[3,4] | Elton J. R. Vasconcelos[3] | Ricardo Perecin Nociti[2] | Ana C. F. C. M. de Ávila[2] | Juliano Rodrigues Sangalli[2] | Igor Garcia Motta[5] | Gilmar Arantes Ataíde Jr[5] | Júlio C. B. da Silva[2] | Yeda Fumie Watanabe[6] | Angela Gonella-Diaza[7] | Juliano C. da Silveira[2] | Guilherme Pugliesi[5] | Flávio Vieira Meirelles[2] | Niamh Forde[1,3]

[1]Discovery and Translational Sciences Department, Leeds Institute of Cardiovascular and Metabolic Medicine, School of Medicine, University of Leeds, Leeds, UK

[2]Departamento de Medicina Veterinária, Faculdade de Zootecnia e Engenharia de Alimentos, Universidade de São Paulo, Pirassununga, Brazil

[3]LeedsOmics, University of Leeds, Leeds, UK

[4]National Heart and Lung Institute, Imperial College London, London, UK

[5]Department of Animal Reproduction, School of Veterinary Medicine and Animal Science, University of São Paulo, Pirassununga, Brazil

[6]Vitrogen – Biotecnologia em Reprodução Animal, Cravinhos, Brazil

[7]North Florida Research and Education Center, Institute of Food and Agricultural Sciences, University of Florida, Gainesville, Florida, USA

Correspondence
Niamh Forde, PhD, Discovery and Translational Sciences Department, Leeds Institute of Cardiovascular and Metabolic Medicine, School of Medicine, University of Leeds, Leeds, UK.
Email: n.forde@leeds.ac.uk

Funding information
UKRI | Biotechnology and Biological Sciences Research Council (BBSRC), Grant/Award Number: BB/R017522/1; Fundação de Amparo à Pesquisa do Estado de São Paulo (FAPESP), Grant/Award Number: 2016/22790-1, 2017/50438-3 and 2018/14137-1

Abstract

We tested the hypothesis that the biosensor capability of the endometrium is mediated in part, by the effect of different cargo contained in the extracellular vesicles secreted by the conceptus during the peri-implantation period of pregnancy. We transferred *Bos taurus taurus* embryos of different origin, in vivo (high developmental potential (IV)), in vitro (intermediate developmental potential (IVF)), or cloned (low developmental potential (NT)), into *Bos taurus indicus* recipients. Extracellular vesicles (EVs) recovered from Day 16 conceptus-conditioned medium were characterized and their microRNA (miRNA) cargo sequenced alongside RNA sequencing of their respective endometria. There were substantial differences in the endometrial response to in vivo versus in vitro and in vivo versus cloned conceptuses (1153 and 334DEGs respectively) with limited differences between in vitro Vs cloned conceptuses (36 DEGs). The miRNA cargo contained in conceptus-derived EVs was similar between all three groups (426 miRNA in common). Only 8 miRNAs were different between in vivo and cloned conceptuses, while only 6 miRNAs were different between in vivo and in vitro-derived

conceptuses. Treatment of endometrial epithelial cells with mimic or inhibitors for miR-128 and miR-1298 changed the proteomic content of target cells (96 and 85, respectively) of which mRNAs are altered in the endometrium in vivo (*PLXDC2, COPG1, HSPA12A, MCM5, TBL1XR1*, and *TTF*). In conclusion, we have determined that the biosensor capability of the endometrium is mediated in part, by its response to different EVs miRNA cargo produced by the conceptus during the peri-implantation period of pregnancy.

KEYWORDS

endometrium, extracellular vesicles, microRNA

1 | INTRODUCTION

In placental mammals, the majority of reproductive wastage occurs in the first 2–3 weeks of pregnancy with a specific wave of loss occurring during the peri-implantation period.[1] Establishing successful early pregnancy requires communication between the gametes and the maternal environment as well as successful bi-directional communication between the developing conceptus (embryo and extra-embryonic membranes) and the uterine environment. Irrespective of the species studied, or indeed the type of conceptus present, there is an optimum window of uterine receptivity (UR) to implantation.[2–4] Furthermore, recent data in multiple species indicate that the endometrium is capable of "sensing" the type of embryo present.[5–7] Studies in mammals with diverse implantation strategies (invasive implantation in humans and superficial implantation in cattle) have shown that embryos with different developmental competencies, i.e., embryos more likely to give rise to successful pregnancy (in vivo produced) versus those that do not (in vitro, clones), are sensed by the endometrium during pregnancy recognition/implantation, and the endometrium modifies its transcriptome accordingly.[5–7] Not only does the endometrium establish UR to implantation, but it also modifies this receptivity depending on the quality of embryo present. However, the mechanism by which the endometrium does this still remains elusive.

In cattle, coordinated with conceptus elongation, the trophectoderm cells produce and secrete increasing concentrations of the pregnancy recognition signal IFNT.[8] In addition to this secretion of IFNT, the conceptus produces additional proteins[4,9–11] that induce transcriptional changes in the endometrium. Interestingly, data from Bauersachs et al.[6] demonstrate that exposure of the endometrium to the conceptus induced a larger transcriptional response than exposure to a type 1 interferon response alone in vivo, i.e., factors other than IFNT alter the endometrial transcriptome. In work by Bauersachs,[12] no changes in IFNT production by embryos with different developmental competencies were determined, therefore, the biosensor capability of the endometrium is not mediated only by the production of different concentrations of IFNT nor subsequent actions on the endometrium.

Recently, extracellular vesicles (EVs) have emerged as a non-traditional form of cell-to-cell communication. EVs are membrane-bound vesicles (classified depending on their size and biogenesis) and contain lipids, proteins, and RNA (both coding and non-coding RNAs) molecules that are capable of being incorporated into target tissues.[13] Data in mouse has show that EVs produced by embryonic stem cells (ESC), are delivered to the trophectoderm lineage to enhance embryo implantation in the endometrium.[14] One of the first reports of this phenomenon in the uterus was through the incorporation of endogenous retroviral envelope proteins that are shed from the endometrial epithelium, and incorporated into the trophectoderm cells of sheep conceptuses, with more recent data confirming that the mode of transfer of these retroviral particles was via EVs (specifically exosomes).[15,16] This phenomenon has been reported in other species, e.g., sheep and cattle at different points on the reproductive axis.[17] More recently, it has been demonstrated that miRNAs from the embryo are detectable in culture media, although it is not clear if these are EV-derived.[18,19] Additionally, bovine blastocysts produced in vivo or in vitro are capable to secrete different amounts of EVs containing different miRNA contents.[20]

The *overarching hypothesis* tested, is that the biosensor capability of the endometrium is mediated in part, by loading of different EV cargo derived from the conceptus during the pregnancy recognition period. To test this hypothesis, we produced embryos from *Bos taurus taurus* individuals with different developmental potential and transferred them into *Bos taurus indicius* recipients to determine how the biosensor capability of the endometrium is mediated.

2 | MATERIALS AND METHODS

Unless otherwise stated, all chemicals were sourced from Sigma. All animal work was carried out at the University of São Paulo Pirassununga with full ethical approval from the local ethical committee (approval number: CEUA 7920220219). All experiments were carried out in three experimental replicates, i.e., three sets of experiments with all three experimental groups represented in each replicate. All recipient animals were from *Bos taurus indicus* (Nelore breed), and all three types of embryos were derived from *Bos taurus taurus* as described below. Animals were between 2 and 5 years old and were managed under good body conditions. Recipients were maintained in *Panicum maximum* pastures and had water ad libitum throughout the experiment. All animals enrolled in the study had their estrous cycles synchronized, and blood samples were taken on 7 and 16 days. All animals were scanned for determining CL active by Doppler ultrasonography on Days 7, 16, and 20.

2.1 | In vivo embryo production

Holstein cows (approximately 2nd parity and between 60 to 120 days post-partum) were scanned to ensure they were undergoing normal estrous cycles. On day −9 all animals received an intramuscular injection (i.m.) of 2 mg of estradiol benzoate (Sincrodiol, Ourofino Saúde Animal, Cravinhos, Brazil), along with an intravaginal progesterone-releasing device containing 1 g of P4 (Sincrogest, Ourofino Saúde Animal). On Day −5, each donor ($n = 17$ total) received serial decreasing i/m. injections of FSH (Folltropin, Vetoquinol, France) 12 h apart (1 & 2: 400 IU, 3 & 4: 300 IU, 5 & 6: 200 IU, 7 & 8: 100 IU). After injection 8, the P4 device was removed, and in the evening of day −1, all animals received an i.m. injection of 0.01 mg of GnRH (buserelin acetate, Sincroforte, Ourofino Saúde Animal). All animals were artificially inseminated on day 0 in the AM and PM using semen from the same bull and ejaculate, as used for IVF embryo production. On day 7, the tail of the donors was swabbed with Ethanol, and a 5 mL injection of lidocaine (company, place) was injected into the coccygeal space, to administer a local anesthetic prior to flushing of the reproductive tract. Both the ipsilateral and contralateral uterine horns were flushed with a total volume of 1 liter of sterile PBS without any additives. This was passed through a collection cup fixed with a nylon filter (75 μm) and transported to the lab. The flush was searched under a stereomicroscope for embryos at the appropriate stage of development (late morula/early blastocyst). Identified structures were graded, and placed in IVF media (detailed below) for 2–3 h prior to embryo transfer.

2.2 | In vitro embryo production

All in vitro embryos used for transfer into recipients were produced by Vitrogen (Cravinhos, SP). In vitro maturation (IVM) was performed in TCM 199 supplemented with 10% FBS, 5.0 μg/mL luteinizing hormone (LH, Lutropia-V, Vetrepharm), 0.5 μg/mL follicle-stimulating hormone (FSH, Folltropin-V, Vetrepharm), 0.2 mM pyruvate and 50 μg/mL gentamycin. After 22 h of IVM, oocytes were in vitro fertilized (IVF) with thawed semen from the same bull and from the same ejaculate, prepared using a Percoll gradient.[21] Fertilization (1×10^6 sperm/mL) was performed in TALP medium, supplemented with 2 μM penicillamine, 1 μM hypotaurine, 250 μM epinephrine and 20 μg/mL heparin. After 18 h of fertilization the presumptive zygotes were mechanically stripped of cumulus cells by successive pipetting and transferred to in vitro culture (IVC) in SOF (synthetic oviduct fluid) medium supplemented with 2.5% FBS, 5.0 mg/mL BSA, 0.2 mM pyruvate and 50 μg/mL gentamycin. All IVM, IVF, and IVC procedures were performed in 100 μL drops (20 oocytes per drop), under mineral oil at 38.5°C in 5% CO_2.

2.3 | Generation of cell lines and SCNT embryo production

To establish fibroblast cell lines for cloned embryos, biopsies of subcutaneous tissue from the tail crease of one male and one female Holstein Friesian calf were collected at the Department of Dairy Cattle of University of São Paulo in the Fernando Costa campus. Biopsy fragments were cut into smaller pieces and digested in collagenase (1 mg/mL) for 3 h at 37°C. Digested tissues were washed and centrifuged at 600*g* for 10 min twice and cultured in vitro, in α-MEM medium containing 20% FBS and 50 μg/mL antibiotic (penicillin and streptomycin). The medium was replaced every two days until the establishment of culture. Fibroblasts were transfected with the DNA constructs using a stable transducer with lentivirus vectors (MGH Vector Core, Boston, MA, USA) to express the genes of interest. The GFP (PalmGFP) constructs were provided by the researcher Charles L. Lai, Department of Neurology and Radiology, Massachusetts General Hospital Harvard Medical School (Lai et al., 2016). Briefly, lentiviral particles were produced by lipofection of 293FT cells (Invitrogen) with Lipofectamine 2000 (Invitrogen). The lipofection was incubated overnight (12–16 h), and after this time, the medium was

completely replaced. Cells were seeded at a rate of 1 $\times 10^5$ cells per well on 6-well plates and 50 μL of the viral concentrate plus 8 ng/mL polybrene (hexadimethrine bromide) was added. Culture medium was replaced every 12 h for 5 days. Cells were then frozen at −80°C in α-MEM medium containing 10% FBS, 10% DMSO, and 50 μg/mL antibiotic, and stored in liquid nitrogen.

2.4 | Flow cytometry and sorting of GFP-positive cells

After transfection, fibroblasts from both cell linages (male and female) were evaluated by flow cytometry to check the percentage of GFP-positive cells. As a negative control, non-transfected fibroblasts from both lineages were used. Briefly, the cells were disaggregated from the plates by enzymatic action (TrypLE Express® – Thermo Fisher) per 5 min. After this time, the cells were centrifuged at 300*g* for 10 min, and the pellet was resuspended in 1 mL of fresh media. The cells were then stained with 10 μg/mL Hoechst 33342 for 15 min. Afterward, cells were evaluated separately using FACSCalibur flow cytometer (BD, Seattle, WA, USA). After sorting, GFP-positive cells were recovered in a new 15 mL sterile tube, centrifuged at 300*g* for 10 min and then were seeded in vitro, for use during the somatic cell nuclear transfer to generate cloned embryos positive for GFP.

2.5 | Somatic cell nuclear transfer

The production of the cloned blastocysts was performed according to Refs [22,23]. Briefly, ovaries were collected from a commercial slaughterhouse, transported to the laboratory in physiological solution (NaCl 0.9%) at 35°C, and supplemented with antibiotics (50 μg/mL penicillin and streptomycin). Follicles 3–8 mm in diameter were aspirated with the aid of 18 Gauge needle and 10 mL syringe, and the recovered oocytes were selected using a stereomicroscope. Only those oocytes with a compact cumulus cell layer and homogenous cytoplasm[24] were used for IVM. Following 18 h of IVM, oocytes were denuded in 2% hyaluronidase, and those with the first polar body (1st PB) were incubated in SOF medium containing 10 μg/mL Hoechst 33342 and 7.5 μg/mL cytochalasin B for 15 min. Micromanipulation was performed using an inverted microscope (Nikon Eclipse *Ti*-e, Tokyo, Japan) equipped with micromanipulators and microinjectors (Narishige, Tokyo, Japan). The 1st PB along adjacent cytoplasm was removed by gentle aspiration using a glass pipette with 15 μm of internal diameter (ES transferTip; Eppendorf, Hamburg, Germany). Before aspiration, the oocytes were quickly exposed under UV filter (440 nm). Enucleated oocytes were reconstructed by the injection of a single fibroblast (control, male-derived GFP-positive, or female-derived GFP-Positive fibroblasts) into the perivitelline space of each oocyte. The oocyte and fibroblast resulting from the manipulation were fused in a fusion chamber (Eppendorf) filled with a fusion solution (0.28 M mannitol, 0.1 mM $MgSO_4$, 0.5 mM HEPES, and 0.05% BSA in H_2O), and subjected to alternating current (0.05 kV/cm for 5 s) and direct current (1.75 kV/cm for 45 μs). The presumptive zygotes were activated (26 h after IVM) using 5 μM ionomycin in TCM HEPES 199 with 0.1% BSA, 0.2 mM sodium pyruvate and 50 μg/mL gentamicin for 5 min, followed by incubation in TCM-HEPES 199 with 3% BSA and in 2 mM 6-dimethylaminopurine (6-DMAP) in SOF for 3 h. After this period, the presumptive zygotes were transferred to the IVC as described above (100 μL drops ±20 zygotes per drop).

2.6 | Embryo transfer

On Day 7 of the estrous cycle, all recipients were scanned by transrectal ultrasonography (Hz, and source) as described above, to ensure the presence of an active CL. Blastocysts from all groups were graded, and only those of grade I were individually loaded into transfer straws containing only 1 blastocyst each. Transfer straws were kept at 37°C in a portable incubator and randomly assigned to recipients.

2.7 | Assay for circulating P4 concentrations

Blood samples were collected on days 7 and 16 from the jugular vein for determination of plasma P4 concentrations. Samples were taken using a 10 mL vacuum tube containing heparin (BD Vacutainer, São Paulo, SP, Brazil). The samples were centrifuged at 3600*g* for 15 min at 4°C and the plasma was stored in the freezer at −20°C for subsequent measurements by a solid-phase RIA kit following the manufacture's protocol (ImmuchemTM Double Antibody Progesterone Kit; Cat. 07e170105, MP Biomedicals, NY, USA). The intra-assay CV was 4.37%, and sensitivity was 0.077 ng/mL.

2.8 | Sample recovery

At day 16 of pregnancy, all reproductive tracts were processed for sample collection within 10 min following

slaughter. Ipsi- and contra-lateral uterine horns were identified, and the reproductive tract was trimmed free of excess tissue to facilitate flushing of the uterine horns with laboratory-grade PBS (pH 7.4). Ten mL of PBS was flushed through the ipsilateral and then contralateral uterine horns. The flush was collected in a sterile petri dish (100 mm), and the presence of an appropriately development conceptus was noted. Once the conceptus was identified, each was cultured individually in 3 mL of SOF media at 38.5°C for 6 h, to allow collection of conceptus-derived EVs as previously described,[4] as well as their contemporary blank. Following culture, the conceptus was removed from the culture media, and the CCM as well as the contemporaneous blanks were processed for EV analysis as described below.

2.9 | Isolation and validation of EVs from conceptus-conditioned medium

Isolation of EVs (<200 nm) was carried at 4°C, unless otherwise stated, by standard differential centrifugation followed by ultracentrifugation as previously described,[25] with minor modifications. Briefly, the CCM samples were centrifuged at 300 *g* for 10 min to remove cellular debris followed by 10 min at 2000 g, and a 30 min spin at 16500 *g* for 30 min to pellet large micro vesicles. The resulting supernatant was filtered through a 0.22 μm sterile syringe filter (Millipore), to remove particles greater than 200 nm, and centrifuged at 100000*g* for 70 min (Beckman Coulter, 70TI rotor, 4 mL polycarbonate tube, cat 355 645). Following centrifugation, the supernatant was discarded, and the pellet was washed with excess PBS (pH 7.4). The washed suspension was centrifuged an additional time at 100000*g* for 70 min to pellet the EV fraction.

2.10 | NanoSight analysis

The resulting EV pellets were resuspended in 50 μL and 100 μL of PBS for characterization, respectively. For size and concentration determination, samples were kept at 4°C, prior to analysis by Nano Tracking Analysis (NTA; NanoSight instrument NS300, Malvern, UK). Videos (5 × 30 s) were acquired after the manual introduction of EV samples (aliquot diluted 1:500 in PBS), at camera level 12, at 38.5°C, and by reference to 50, 100, and 150 nm calibration beads (Malvern) to verify accuracy. The EV samples were preserved at −80°C until further use. EV size and concentration between groups were compared on R (R version 3.6.3) using an ANOVA (function aov). Data were plotted using ggplot2 in R.

2.11 | Transmission electron microscopy

Transmission electron microscopy (TEM) was performed to visualize the size and morphology of the EVs contained in the CCM of the conceptuses (IV, IVF, and NT). For this, the EVs from CCM (1 mL) from each group were isolated by ultracentrifugation (100 000 *g* 70 min at 4°C) as previously described. The resulting pellets with the EVs were fixed with 2.5% glutaraldehyde, 0.1 M cacodylate, and paraformaldehyde 4% (pH 7.2 to 7.4) for 2 h at RT. Afterward, ultracentrifugation was performed, the EVs pellets were resuspended in ultrapure water (Milli-Q; Millipore Corporation, Merk, Burlington, MA, USA) and the samples were ultracentrifuged again. The isolated EVs were diluted in 50 μL of ultrapure water and placed on a copper grid coated with Pioloform® (Scientific Agar, Essex, UK) for 5 min. The grid was immediately placed in a drop of 2% aqueous uranyl acetate for 3 min. Excess solution was removed and the reading was performed in a transmission electronic microscope (FEI 200 kV model Tecnai20 emitter LAB6).

2.12 | Imaging and confirmation of GFP in conceptus and endometrial samples

Conceptus GFP-positive was visualized on the inverted phase contrast microscope (Nikon Eclipse TS100, Tokyo, Japan) at 10× magnification and quick exposure time for the conceptus both prior to and after 6 h culture. Endometrial samples from GFP clone were also analyzed for GFP incorporation and endometrium counter-stained with DAPI, (358 nm) and visualized using the epifluorescence microscope (Carl Zeiss, Thornwood, NY) with FITC filters (448 nm) and 400 ms exposure times. PCR analysis and Western blot for the GFP insert were carried out on endometrial samples as follows. The samples of CCM (1 mL) from conceptuses (IV, IVF, and NT) were ultracentrifuged, as previously described in the manuscript, and the resulting pellet was evaluated for the presence of specific protein marker of EVs (endosome pathway marker): ALIX (1:750, sc49267, Santa Cruz Biotechnology, Dallas, TX, USA). As a negative marker, the protein GRP78 (1:1000, sc-166 490, Santa Cruz Biotechnology, Dallas, TX, USA) was used. Briefly, after ultracentrifugation, the pellet containing the EVs was resuspended in 50 μL of RIPA buffer. Laemmli buffer and 2-mercaptoethanol were added to the samples (1:4) which were then denatured at 95°C for 5 min. For each Western blot analysis, 12 μL of each sample was loaded onto 8% SDS-polyacrylamide gels and the run was performed at 100 V for 2 h. Proteins were transferred to a nitrocellulose membrane (#1620112 Bio-Rad) using Bio-Rad products and system for 2 h at 80 V.

Membrane blocking was performed with 5% BSA (Sigma-Aldrich) in Tris-buffered saline (1X – TBST; 100 mM NaCl, 0.1% Tween 20 and 50 mm Tris, pH 7.4) for 1 h. Afterward, the membranes were incubated overnight at 4°C with the primary antibodies, in 1X-TBST containing 1% BSA. The next day, the blots were washed three times for 5 min with 1X-TBST in a shaker, and incubated with HRP-conjugated secondary antibody diluted in 1X-TBST (1:2000) for 1 h at RT. At the end of this period, the membranes were washed three more times with 1X – TBST, and treated with Clarity™ Western ECL substrate (Bio-Rad) for protein visualization.

2.13 | EV RNA extraction and sequencing

RNA was extracted using the Qiagen miRNeasy kit (Qiagen, UK) and the Qiagen MinElute Cleanup Kit (Qiagen, UK) following the manufacturer's instructions. A total of 700 µL of QIAzol (Qiagen, UK) were added directly to the EV samples. After 5 min incubation, 140 µL of chloroform was added, samples shaken vigorously for 15 s, and then incubated for 3 min at RT. The tubes were centrifuged for 15 min at 12000*g* at 4°C to separate the phases. Three hundred and fifty µL of 70% ethanol was mixed with the aqueous phase by vortexing, applied to an RNeasy Mini Spin column, and centrifuged for 15 s at 8000*g*. The membrane was preserved at 4°C for >200 nt RNA extraction. The flow through containing <200 nt RNA was mixed with 450 µL of 100% ethanol and vortexed. The mix was added to an RNeasy MinElute Spin column and centrifuged for 15 s at 8000*g*. The membrane was then washed with 500 µL of RPE buffer and centrifuged for 15 s at 8000*g* and washed again with 500 µL of 80% ethanol. The ethanol was removed, and the membrane dried for 2 min at 8000 g. The membrane was finished drying by a 5 min spin at 8000 *g*, with the lid open. Finally, the RNA was eluted in 14 µL of RNase-free water for 1 min at 8000 *g* and the membrane was re-eluted with the flow through, snap-frozen, and stored at −80°C until further processing.

2.14 | Sequencing of small RNA species in EVs

All the RNA sequencing analysis was performed by Novogene (Cambridge, UK). Briefly, 3′ and 5′ adaptors were ligated to 3′ and 5′ end of small RNA, respectively. Then the first strand cDNA was synthesized after hybridization with reverse transcription primer. The double-stranded cDNA library was generated through PCR enrichment. After purification and size selection, libraries with insertions between 18 and 40 bp were ready for sequencing on Illumina sequencing with SE50. The library was checked with Qubit and real-time PCR for quantification and bioanalyzer for size distribution detection. Quantified libraries will be pooled and sequenced on Illumina platforms, according to effective library concentration and data amount required.

2.15 | Analysis of the miRNA cargo of EVs

Data were analyzed through the LeedsOmics pipeline for small RNA sequencing. For the <200 nt samples, adapter trimming, quality trimming, and filtering were performed using Cutadapt.[26] We used Bowtie[27] to align the reads onto the *Bos taurus* reference genome (Btau_5.0.1) downloaded from the NCBI Assembly database,[28] SAMtools to convert the SAM files into BAM files,[29] and sort and index BAM files, featureCounts[30] to quantify the reads according to the *Bos taurus* microRNAs annotation file in GFF3 format collected from the miRBase database (v22)[31] and DESeq2 to identify the differentially expressed miRNAs.[32] The differentially expressed miRNAs were filtered for a $\log_2$FoldChange >1 (or <−1) and an adjusted *p*-value < .05.

2.16 | Target prediction

miRNA targets were predicted on TargetScan (targetscan.org; version 7.2). The list of predicted targets for each miRNA was retrieved and filtered for Cumulative weighted context++ score ≥ −0.5, as the lower the score, the more likely the miRNA targets the gene. Finally, the list of targets was compared between groups on Venny (https://bioinfogp.cnb.csic.es/tools/venny/; version 2.1). bta-miR-12034 could not be searched on TargetScan as it is not present on the miRNA database of the website.

2.17 | Endometrial RNA extraction and sequencing

RNA from endometria exposed to in vivo ($n = 6$), in vitro ($n = 10$), or cloned ($n = 10$) conceptuses was extracted using the Qiagen mini miRNeasy kit (Qiagen, UK) and the Qiagen MinElute Cleanup Kit (Qiagen, UK) following the manufacturer's instructions. A total of 700 µL of QIAzol (Qiagen, UK) were added directly to the tissue samples, and homogneized thoroughly using a TissueRuptor (Qiagen, UK) for 15–90 s. After 5 min incubation, 140 µL of chloroform was added, samples shaken vigorously for 15 s, and then incubated for 3 min at RT. The tubes were centrifuged for 15 min at 12000*g* at 4°C to

separate the phases. Three hundred and fifty μL of 70% ethanol was mixed with the aqueous phase by vortexing, applied to an RNeasy Mini Spin column and centrifuged for 15 s at 8000*g*.

The membranes binding the >200 nt RNA were washed with 350 μL RWT buffer for 15 s at 8000 g. Then the membranes were DNase treated (DNase I, Qiagen) for 15 min at room temperature. After this, they were washed with 300 μL of RWT buffer for 15 s at 8000 g. Two more consecutive washes with 500 μL of RPE buffer were performed for 15 s at 8000 g before drying the tube for 1 min at 16100 g with the lid open. The RNA was eluted with 50 μL of RNase-free water for 1 min at 16100 g. The membrane was re-eluted a second time with the flow through. At this point, samples were quantified using a NanoDrop and then snap-frozen and stored at −80°C until further processing.

2.18 | Sequencing of >200 nt RNA species in endometrium

All the RNA sequencing analysis was performed by Novogene (Cambridge, UK). Firstly, ribosomal RNA was removed by rRNA removal kit, and rRNA-free residue was cleaned up by ethanol precipitation. Subsequently, sequencing libraries were generated using the rRNA-depleted RNA and performing procedures as follows. Briefly, after fragmentation, the first strand cDNA was synthesized using random hexamer primers. Then the second strand cDNA was synthesized and dUTPs were replaced with dTTPs in the reaction buffer. The directional library was ready after end repair, A-tailing, adapter ligation, size selection, USER enzyme digestion, amplification, and purification. The library was checked with Qubit and real-time PCR for quantification and bioanalyzer for size distribution detection. Quantified libraries will be pooled and sequenced on Illumina platforms, according to effective library concentration and data amount required.

2.19 | Bioinformatics analysis endometrial RNA

The adapter sequences trimming and quality filtering of the samples >200 nt were performed by Cutadapt implemented in the Trimgalore pipeline.[26] Sequencing reads of each sample were aligned using STAR[33] with standard parameters for alignment with the *Bos taurus* genome (Ensembl *Bos taurus* ARS-UCD1.2), and gene count was analyzed using featureCounts[30] implemented in the Rsubread package.[34] Genes were considered expressed when they presented more than 5 counts in at least 70% of samples per group. Differential gene expression analysis was performed using the DESeq2 package,[32] considering significance when the adjusted p values were less than 0.1 (Benjamini-Hochberg – "BH") and the module of $\log_2$ foldchange was greater than 1. Additionally, we considered genes as differentially expressed if they were exclusively expressed in one group (at least 5 counts in all technical replicates), and not expressed in the other group (zero counts in all technical replicates) within comparison and using the function filterByExpr from edgeR package.[35] Gene ontology analysis was performed using clusterProfiler[36] and pathways explored using Pathview.[37] Data were visualized using R software, in which we primarily observed the classification, intensity, and difference in expression between groups. Exploratory data analysis was performed with principal component analysis using plotpca function from DESeq2[34] and ggplot2 package,[38] smearplots built with ggplot2,[38] heatmaps using Ward.D2 clusterization method from pheatmap package.[39]

2.19.1 | Functional analysis of selected miRNA on endometrial expression

miRNA mimic & inhibitor transfection

Primary bovine endometrial epithelial cells ($n = 3$) isolated as previously described[11] were plated at 50000 cells/well in a 24-well plate. The cells were incubated in a 5% CO_2 environment at 38.5°C in 2 mL RPMI 1640 media (Gibco, UK) with 10% FBS (Gibco One-Shot FBS, UK) (charcoal stripped to deplete hormones), and 1% ABAM (Gibco, UK). Seventy-two hours after seeding, the cells were washed in PBS and the media was replenished with 450 μL RPMI media with EV-depleted charcoal-stripped FBS (Gibco One-Shot exosome-depleted FBS, UK) without antibiotics per well. The cells were transfected with the optimal concentration of 2 μL of Lipofectamine 3000 (Invitrogen, UK) and 200 nM mimic/inhibitor (Horizon Discovery, UK) per well. The experimental design comprised a control (50 μL) OptiMEM only (Gibco, UK), a vehicle control (2 μL Lipofectamine 3000 in 50 μL OptiMEM), a mimic and an inhibitor of each miRNA studied (miR-128 and miR-1298), a non-targeting mimic, and a non-targeting inhibitor. Briefly, per well, 2 μL of 100uM mimic/inhibitors were mixed with 18 μL OptiMEM, then further diluted by taking 10 μL and adding a further 15 μL OptiMEM (resulting concentration 4 μM). Two μL of Lipofectamine was mixed with 250 μL of OptiMEM medium, and incubated for 5 min at RT. After the incubation, the Lipofectamine solution (25 μL) was individually mixed with the targeting/non-targeting mimic/inhibitor solution (25 μL), and after a 20 min incubation at room temperature, they were added to the corresponding wells. The cells were collected 48 h after treatment by

lifting with trypsin (0.025% for 5 min), neutralizing with medium and pelleted at 500 g for 5 min. Cells were then re-suspended in PBS, re-pelleted at 500 × g for 5 min, and the cell pellet snap-frozen prior to proteomic analysis.

Proteomic analysis

Cell pellets were placed on ice, and resuspended in 40 µL RIPA buffer 1X (Merck, UK) with added cOmplete ULTRA protease inhibitors (Roche, UK), vortexed briefly, and kept on ice for 20 min. Samples were then centrifuged for 15 min at 14000 g at 4°C and supernatant transferred to Eppendorfs alongside a sample of lysis buffer for proteomics analysis. Tandem mass Tag labeling and high pH reversed-phase chromatography was carried out as previously described,[40] by the University of Bristol core facility with minor modifications. These raw data files were processed and quantified using Proteome Discoverer software v2.1 (Thermo Scientific) and searched against the UniProt *Bos taurus* database (downloaded October 2021: 37512 entries) using the SEQUEST HT algorithm. The peptide precursor mass tolerance was set at 10 ppm, and MS/MS tolerance was set at 0.6 Da. The search criteria included oxidation of methionine (+15.995 Da), acetylation of the protein N-terminus (+42.011 Da), and methionine loss plus acetylation of the protein N-terminus (−89.03 Da) as variable modifications and carbamidomethylation of cysteine (+57.021 Da) and the addition of the TMT mass tag (+229.163 Da) to peptide N-termini and lysine as fixed modifications. Searches were performed with full tryptic digestion and a maximum of 2 missed cleavages were allowed. The reverse database search option was enabled and all data was filtered to satisfy false discovery rate (FDR) of 5%. Overrepresentation analysis was carried out using G profiler (https://biit.cs.ut.ee/gprofiler/gost) to understand what overrepresented pathways, cell components, biological process, and molecular functions were modified by these microRNAs in vitro.

3 | RESULTS

3.1 | Animal model and EV characterization

Following production of in vivo, in vitro, and cloned *Bos taurus taurus* embryos, blastocysts were transferred into synchronized *Bos taurus indicus* recipients (Figure 1). Fibroblasts from both cell linages (male and female) were evaluated by flow cytometry with 79.6% of cells positive for GFP and 64.4% of cells positive for GFP in the female line (Figure S1). Concentrations of plasma progesterone (P4) in recipients on the day of embryo transfer (day 7) or

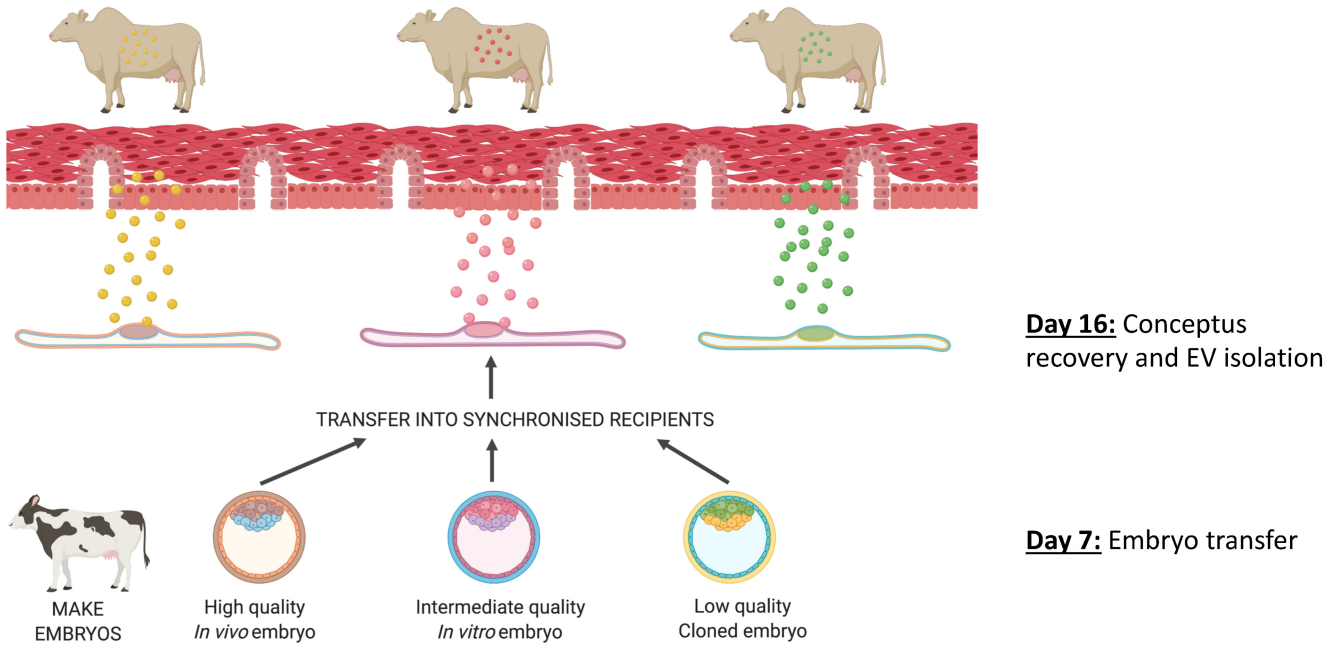

FIGURE 1 Schematic diagram of animal model. We tested the hypothesis that the biosensor capability of the endometrium is mediated in part by different cargo present in extracellular vesicles produced by the conceptus during the pregnancy recognition period. To test this hypothesis, *Bos taurus taurus* embryos were produced to generate both male and female high-quality in vivo embryos (gold), intermediate-quality in vitro embryos (pink), or low-quality cloned embryos (green). Embryos were transferred into synchronized *Bos taurus indicus* recipients, and conceptuses and endometrial tissue were recovered on Day 16, cultured for 8 h, and extracellular vesicles (EVs) characterized and cargo examined.

at slaughter (day 16) did not differ ($p > .1$) among groups (Figure 2A) nor between day 7 and day 16. On Day 16, 28 conceptuses were recovered from recipients. Sexing of the conceptuses revealed six in vivo-derived conceptuses (IV: 3 females, 3 males), 10 in vitro-derived (IVF: 7 females, 3 males), and 12 cloned conceptuses (NT: 5 females, 7 males; Figure S2). In cloned embryos, green fluorescent protein (GFP) was detected in fibroblast cells (Figure 2B), blastocysts prior to transfer (Figure 2C), and recovered conceptuses (Figure 2D), fibroblast and conceptuses (Figure 2E) as well as adjacent to the LE of the endometrium on Day 16.

Analyses of EVs derived from conceptus conditioned medium (CCM) revealed no difference in particle concentration (mean concentration 2.15 $\times 10^9$ particles/mL; in vivo: 1.11 $\times 10^9$, in vitro: 2.14 $\times 10^9$, and clones; 2.69 $\times 10^9$ particles/mL, Figure 3A), nor size (in vivo: 155.35 nm ($\pm$12.86 nm), in vitro: 159.14 nm ($\pm$13.55 nm), and clones; 171.2 nm ($\pm$23.45 nm) (Figure 3B)). Western blot analysis of markers of EVs detected ALIX in our isolated EVs from in vitro and cloned conceptuses but not from in vivo derived EVs, similar to previously reported data.[20] but the absence of GRP78 (Figure 3C), while TEM demonstrated classical EV shape (Figure 3D,E).

3.2 | The endometrium responds differently to conceptuses with different developmental potential and sex

To determine if the endometrium responds to conceptuses with different developmental competencies, we performed RNAseq analysis on the intercaruncular endometrium of recipients on Day 16 of pregnancy. In total 18 077 transcripts containing more than >200 nucleotides with a count >5 were detected in the endometrium. Heatmap analysis demonstrated the overall transcriptional profile of endometrium clustered according to developmental competency of the conceptus to which it was exposed (Figure 4A). Endometria exposed to in vivo conceptuses, compared to in vitro produced conceptuses on Day 16, displayed altered expression of 1153 transcripts (differentially expressed genes – DEGs: 926 of which were upregulated, 227 downregulated: Table S1). Overrepresented pathways associated with all 1153 DEGs, i.e., irrespective of the direction of change, are involved in molecular functions of integrin binding and cell adhesion molecule binding (Table S2), while overrepresented pathways included MAPK signaling pathway, Focal adhesion, and Wnt signaling pathway (Table S3). Of the

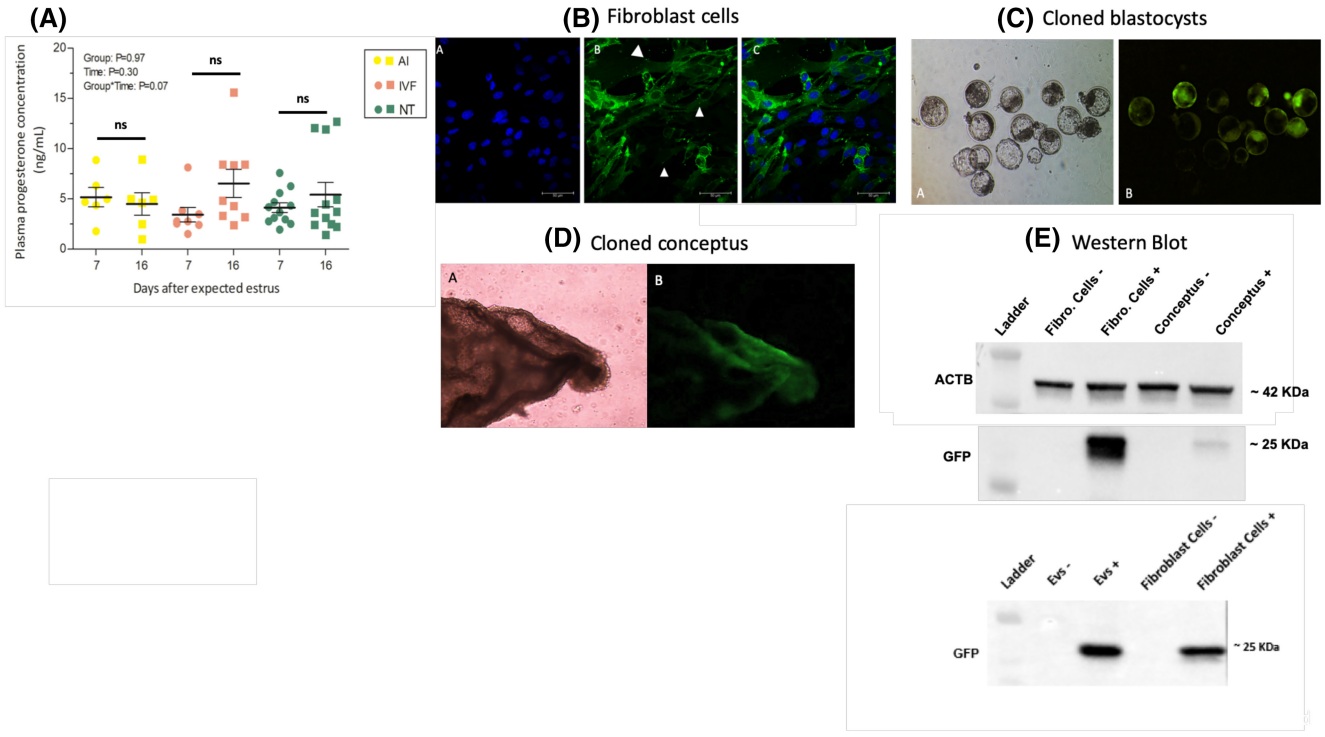

FIGURE 2 Animal model validation. (A) Plasma progesterone concentrations measured on Day 7 (day of embryo transfer) and Day 16 (day of maternal recognition of pregnancy) in recipient animals where in vivo (yellow), in vitro (pink), or cloned (green) embryos were transferred. (B) Representative image of GFP present in fibroblast cells used to generate cloned embryos. GFP-expressing (C) blastocysts and (D) day 16 conceptuses. (E) Western blot probing for GFP in fibroblast cells and conceptuses.

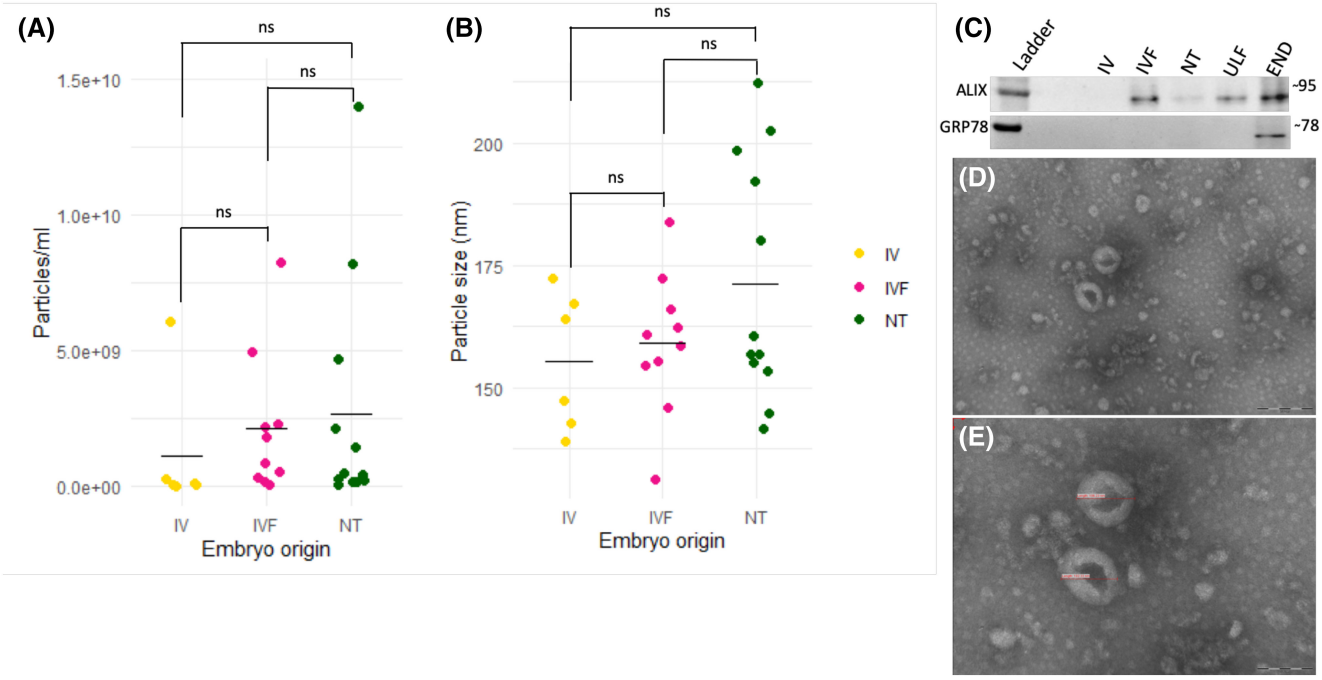

FIGURE 3 Characterization of EVs derived from conceptuses. (A + B) Nano-particle tracking analysis of EVs derived from Day 16 CCM from in vivo (yellow), in vitro (pink), or cloned (green) conceptuses. No difference in (A) particle number concentration or (B) size of EVs was detected. (C) Western blot analysis of EV markers of EVs ALIX and GRP78 in EVs from IVF, NT, ULF, and endometrium. (D + E) TEM of the same representative EVs from IVF conceptuses demonstrating the expected size and classical EV shape. Panel D is taken using 100 000× magnification (scale bar 200 nm) while the sample field is represented in panel E using 200 000× magnification (scale bar 100 nm).

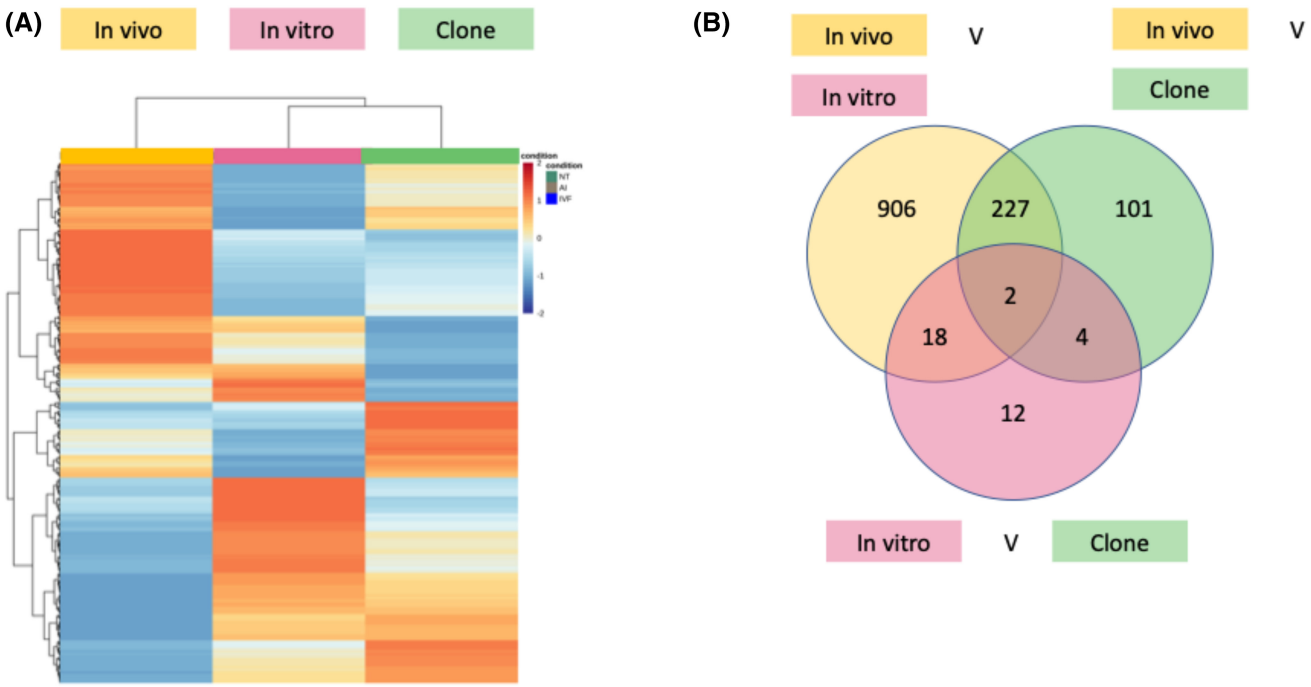

FIGURE 4 Endometrial response to conceptuses with different developmental competencies. (A) Heatmap analyses of transcriptomic response (measured by bulk RNA sequencing) of the endometrium on Day 16 of confirmed pregnancy following transfer of embryos with different developmental competencies on Day 7 to synchronized recipients. Specific clustering of the transcriptional response is observed for endometria exposed to high-quality in vivo-produced embryos (LHS, gold color ($n = 6$), intermediate-quality in vitro embryos (middle, pink color ($n = 10$), or low-quality embryos (RHS, green color ($n = 10$) confirming the biosensor capability of the endometrium previously proposed by Refs [5,6,41] (B) Venn diagram with the numbers of differentially expressed genes identified between endometria exposed to embryos with different developmental competencies (IV, IVF, and NT).

up-regulated transcripts, Oxytocin signaling pathway, hedgehog signaling, and ECM-receptor interactions were overrepresented (Table S4), as well as the molecular function ontology of integrin binding (Table S5). In contrast, the down-regulated genes (in vivo vs. in vitro) were associated with biological processes of positive regulation of secretion by cell, secretory pathway, and positive regulation of exocytosis (Table S6) with genes overrepresented in pathways involved in MAPK signaling pathway, Oxytocin signaling pathway, Ras signaling pathway, and Focal adhesion (Table S7).

Exposure of the endometrium to in vivo (high-quality) compared to cloned embryos (low developmental potential) altered 334 transcripts of which 291 were upregulated and 43 downregulated (Table S8). These were associated with molecular functions of voltage-gated potassium channel complex and potassium channel complex (Table S9) and pathways including Axon guidance, calcium signaling pathway, and MAPK signaling pathway (Table S10).

In contrast, only 36 DEGs were altered in endometrium exposed to in vitro and cloned conceptuses (Table S11), all of which were upregulated in in vitro-exposed endometrium and are overrepresented in biological process including protein/peptide transport (Table S12), an pathways of Drug metabolism – cytochrome P450, and Glutathione metabolism (Table S13). Embryos produced by assisted reproductive technologies altered a consistent signature of 227 DEGs (Figure 4B; Table S14) compared to in vivo-produced embryos, but were not associated with any overrepresented categories. While only 2 genes were different in all three groups (Figure 4B. *CHSY3*; chondroitin sulfate synthase 3, and *SLC24A3*; solute carrier family 24 member 3). We also determined that, irrespective of the type of conceptus present the sex of the conceptus altered the transcriptional response independently (Figure 5).

3.3 | Small RNA sequencing of conceptus-derived EVs

To understand if there are differences in miRNA cargo of EVs, we sequenced the composition of micro RNAs in EVs. In total, 314 miRNAs were present as cargo in day 16 conceptus-derived EVs (Figure 6; Table S15). Three hundred and fifty-nine, 321, and 384 miRNAs were identified in EVs derived from in vivo, in vitro, and cloned conceptuses, respectively. Of these, 317 were common to all the 3 groups and 29 were unique to cloned conceptuses. Cloned conceptuses shared similar miRNA EV cargo with in vivo (43 miRNAs) and in vitro-produced conceptuses (114 miRNAs) (Figure 6). Filtering of these miRNAs to those with a $\log_2$FoldChange >1 (or <−1), and an adjusted

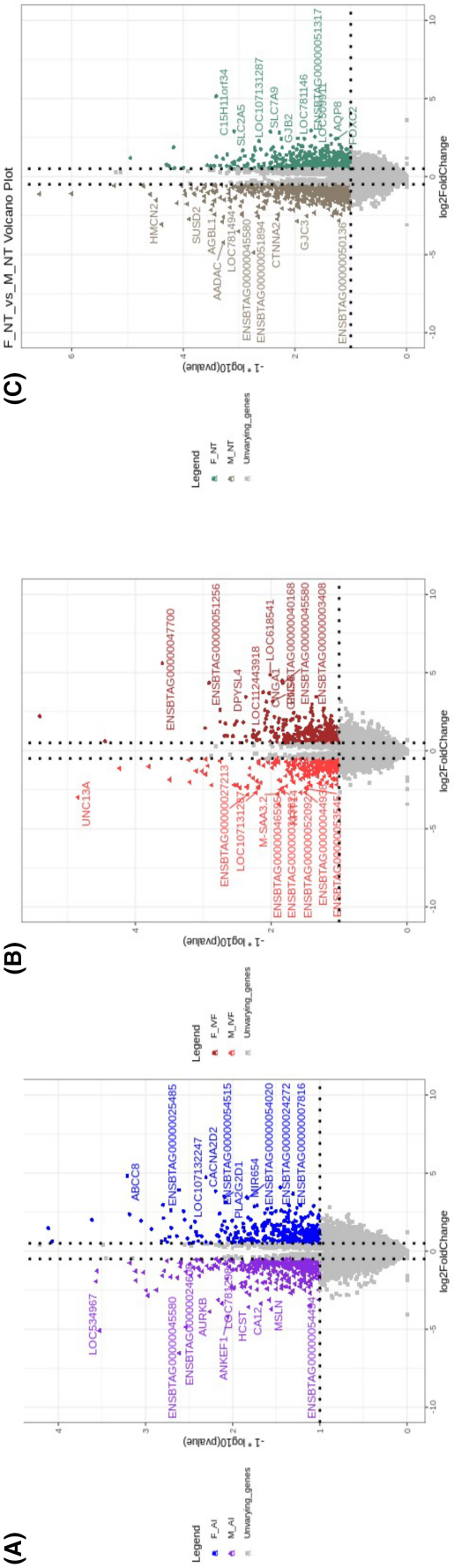

FIGURE 5 Endometrial response to conceptuses with different developmental competencies. Volcano plots showing differences in transcriptional response of the endometrium to male compared to female conceptuses produced (A) in vivo, (B) in vitro, or (C) cloned conceptuses on Day 16 of pregnancy.

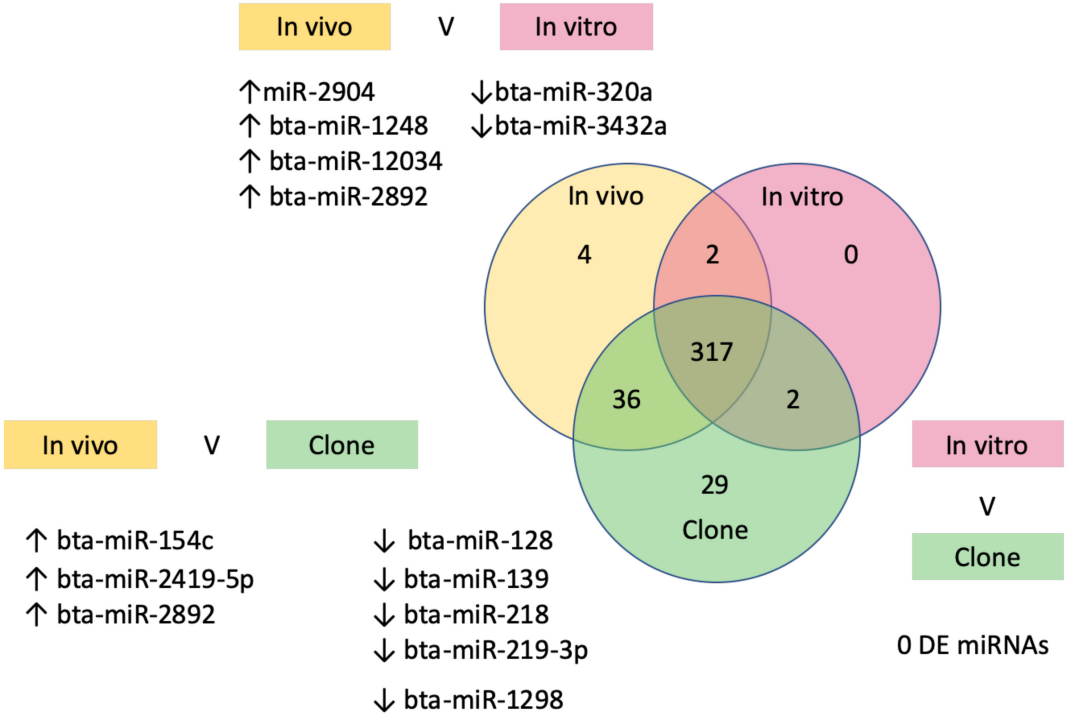

FIGURE 6 Micro RNA cargo of EVs from Day 16 conceptuses. Venn diagram analyses of miRNA cargo of EVs isolated from CCM. Media was derived from in vivo, in vitro, or cloned conceptuses cultured in vitro for 8 h. EVs were characterized as per ISEV guidelines, and miRNA profiling was carried out via miRNA sequencing.

p-value of < .05, identified no significant differences in miRNA cargo from EVs derived from conceptuses produced in vitro or via cloning. In contrast, 6 miRNAs were differentially expressed in EVs derived from in vivo compared to in vitro conceptuses, 2 of which were downregulated (bta-miR-320a and bta-miR-3432a) and 4 upregulated (bta-miR-1248, bta-miR-2892, bta-miR-2904, and bta-miR-12034). In total, 8 miRNAs were differentially abundant in EVs from in vivo compared to cloned conceptuses, 5 downregulated (bta-miR-128, bta-miR-139, bta-miR-218, bta-miR-219-3p, and bta-miR-1298) and 3 upregulated (bta-miR-154c, bta-miR-2419-5p, and bta-miR-2892).

3.4 | Functional analyses of selected EV-miRNAs

We selected miR-128 and miR-1298 for further analysis as these were EV-derived miRNA with the largest fold change difference between embryos with the most divergent developmental competency, i.e., in vivo and clones. Following the removal of off-target effects, treatment of primary bovine endometrial epithelial cells with miR-128 mimic altered expression of 863 proteins, while treatment with inhibitor altered 562 (Figure 7; Table S16). A core of 96 proteins was modified by both the miR-128 mimic and inhibitor. Of these core proteins overrepresentation analysis revealed these are significantly associated with six molecular functions (including actin binding, and ion binding), four biological processes (actin filament-based movement, DNA damage response, signal transduction by p53 class mediator, movement of cell or subcellular component, and actin filament-based process), 19 cell components (including actin cytoskeleton and vesicle), and one pathway RHO GTPase cycle (Full details of proteins are provided in Table S18).

Of the proteins altered by miR-128 in vitro, the expression of 9 proteins increased, and 2 decreased with their corresponding transcripts also altered in endometria exposed to cloned Vs in vivo conceptuses. One protein (plexin domain containing 2 (PLXDC2)) modified by miR-128 mimic and inhibitor in vitro and also increased in expression in endometria exposed to in vivo versus cloned conceptuses on Day 16.

For miR-1298, removal of off-target effects revealed 949 proteins modified by mimic treatment alone, while inhibitor treatment altered 562 of which 85 were common to both treatments (Figure 8; Table S19). Of these, 85 proteins core proteins overrepresentation analysis revealed these are significantly associated with sixteen molecular functions (including ATP binding, and adenyl ribonucleotide binding), two biological processes (negative regulation of mRNA splicing, via spliceosome and

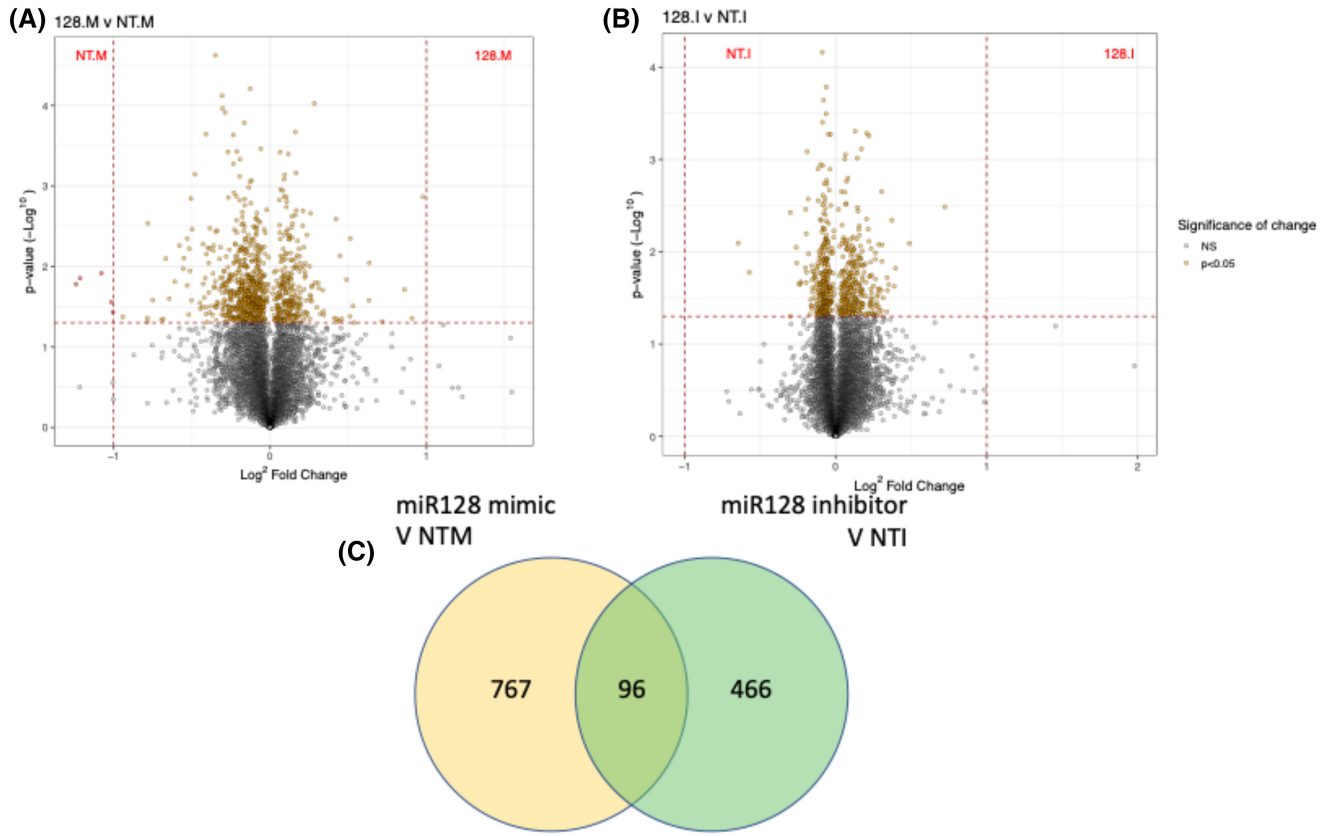

FIGURE 7 In vitro regulation of proteins by miR128. Volcano plots demonstrating differentially abundant proteomic analysis of bovine endometrial epithelial cells transfected with (A) non-targeting mimic or miR-128 mimic or (B) non-targeting inhibitor or miR-128 inhibitor for 48 h ($n = 3$ biological replicates). (C) Venn diagram analysis of common and mimic/inhibitor specific proteomic changes. Differences were determined by tandem mass tag mass spectrometry analysis of protein lysates from the cells.

negative regulation of mRNA processing), and 11 cell components (including intracellular anatomical structure and cytoplasm). We also determined these proteins are overrepresented in two KEGG pathways ((Spliceosome, and Non-small cell lung cancer) and two reactome pathways (Initiation of Nuclear Envelope (NE) Reformation, and Nuclear Envelope Breakdown), Full details of proteins are provided in Table S20). Of the proteins whose abundance was altered by miR-1298, expression of mRNA for 5 of these proteins also changed in the endometrium (COPG1, HSPA12A, MCM5, TBL1XR1, and TTF2). There was minimal overlap in proteins regulated by these miRNAs indicating miRNA specificity in terms of their targets and minimal numbers of these are identified as predicted targets (miRGene DB punch out to Targetscan identified 161 predicted targets for bovine miR-1298).

4 | DISCUSSION

The biological phenomenon that the endometrium acts as a biosensor of embryo developmental competency has been known for over a decade, however, the mechanism by which this is mediated has been elusive. We tested the hypothesis that differences in the cargo of EVs derived from conceptuses with different developmental potential are responsible for the biosensor capabilities of the endometrium. We have clearly demonstrated that the endometrium responds differently to embryos produced by assisted reproductive technologies and these differ depending on how the embryo is produced (Figure 4). These differences are also modified depending on the sex of the conceptus, extending this biosensor capability of the endometrium not only to developmental competency but to conceptus sex also. Following the characterization of EVs from conceptuses during the pregnancy recognition period, differences in the miRNA cargo of EVs were determined. Treatment of endometrial epithelial cells with miRNA mimics and inhibitors for selected miRNAs altered the proteomic composition of the cells, proving for the first time that different miRNAs cargo from conceptus-derived EVs are responsible in part for the biosensor capability of the endometrium.

A major factor that can influence the response of the endometrium to the conceptus is via the actions of P4 on the endometrium which can alter the developmental

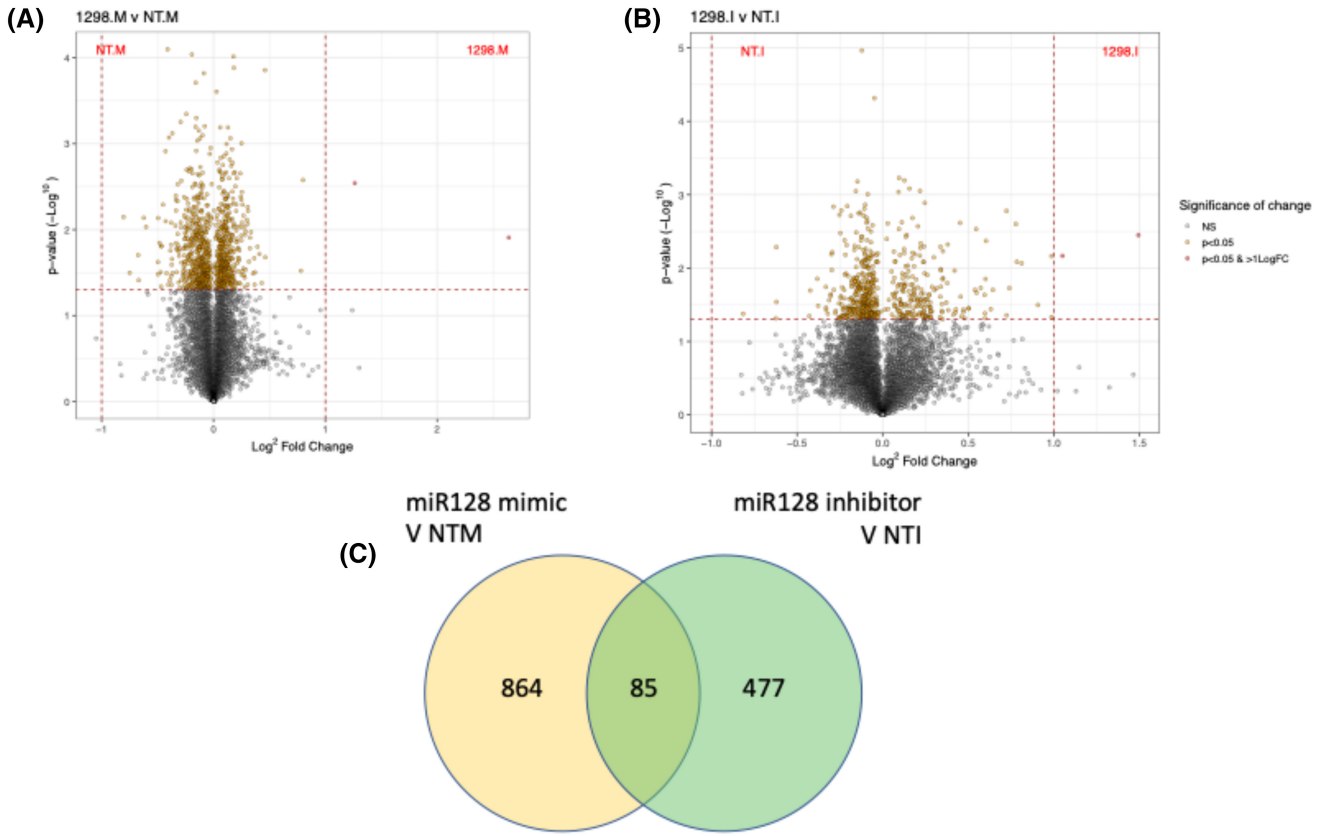

FIGURE 8 In vitro regulation of proteins by miR1298. Volcano plots demonstrating differentially abundant proteomic analysis of bovine endometrial epithelial cells transfected with (A) non-targeting mimic or miR-1298 mimic or (B) non-targeting inhibitor or miR-1298 inhibitor for 48 h ($n = 3$ biological replicates). (C) Venn diagram analysis of common and mimic/inhibitor specific proteomic changes. Differences were determined by tandem mass tag mass spectrometry analysis of protein lysates from the cells.

trajectory of the conceptus.[42] In order to exclude this as a confounding factor from our study we measured concentrations of P4 in the recipients. No differences were observed in the concentration of this key molecule (P4) that regulates the endometrial landscape. Therefore, any differences observed in the endometrial response are not due to the enhanced[43] or delayed[44,45] P4 alterations of the endometrium or ULF composition.[4,46] In vitro culture of the conceptus could lead to the identification of components of EVs (including miRNAs, proteins lncRNAs and mRNAs) that may be an artifact of the culture conditions in this study. In order to reduce this possibility, we have accurately characterized EVs according to current ISEV guidance.[47] Moreover, previous work has shown that conceptus-derived proteins do have a functional effect on the endometrium,[4,11,48] demonstrating that there are functional roles for these proteins identified in conceptus-conditioned medium (CCM). We are confident that these miRNAs may be modifying the endometrium given our data but also additional evidence from previous studies that cargo of extracellular vesicles they are derived from one tissue type can modify target tissue transcriptomic and proteomic landscape.[49] Specifically, signals and conceptus-derived EVs and their cargo can be integrated into the endometrium and alter the transcriptomic/proteomic response in a variety of species in the peri-implantation period of pregnancy. In cattle, EVs from the pregnant ULF, i.e., derived from both the conceptus and endometrium, modify the bovine endometrial epithelial cellular transcriptome[50] and proteome.[51] The actions of pregnancy recognition signals from the conceptus in the pig (PGE2 and E2) alter the biogenesis of EVs in the pig endometrial epithelia cells[52] while[53] show stimulation by miRNAs of conceptus-derived EVs. Different EV cargo, including microRNAs, were detected in the uterine fluid that had targets modified in the endometrium during the peri-implantation period of pregnancy in the pig.[52] Additional papers in other species have demonstrated that conceptus-derived EVs and their cargos modify the endometrial transcriptome.[54–56] We therefore propose that some of the biosensor response of the endometrium is mediated by these different miRNA cargos contained in the EVs from conceptus with different developmental competencies. The differences observed are therefore due to differences in composition of the EVs themselves as no changes in

size, concentration, or indeed markers were observed in EVs from different source conceptuses.

Our study has independently confirmed that the endometrium is a biosensor of developmental potential of the embryo mediated by EVs, as well as identified transcripts that are ART-specifically induced in the endometrium (Figure 4B). Moreover, we have shown that during the pregnancy recognition period the endometrium is also capable of deciphering between male and female conceptuses on Day 16 something not previously reported.[57] Data in several mammalian species have shown embryos produced using different assisted reproductive technologies have different developmental potential and pregnancy outcomes.[1,5,6] For the first time, our evidence demonstrates that these are potentially mediated via differences in embryo-maternal cross-talk during the peri-implantation period of pregnancy. While we know this bi-lateral talk is necessary to support conceptus elongation,[46,58] and required to signal pregnancy recognition, these data support the notion that more nuanced interactions occur with continuous fine-tuning of the necessary secretion from the endometrium that is tailored to the needs (in terms of development) by the conceptus. Despite substantial differences in the transcriptome of the conceptus as it transitions from the blastocyst to an elongated conceptus,[59] there has been limited data on the endometrial response to the sex of the conceptus.[60] Our data show that there is endometrial sensitivity to male and female conceptus during the pregnancy recognition period.

By using an in vitro approach to transfect cells with selected mimics and inhibitors for selected miRNAs that are altered in conceptus-derived EV cargos, we have determined what key pathways in the endometrium that are altered via differences in EV cargo during pregnancy recognition. There are also likely differences in other cargo components. The majority of pathways altered are involved in the secretion and internal cell signaling. This may indicate that not only is the endometrium a biosensor, but that conceptus-derived EVs could potentially alter the endometrial secretome. Overrepresentation analysis of the proteins modified by miR128 in bovine epithelial cells in vitro showed protein-, actin-, and ion binding as molecular functions while the proteins localized to cytoskeleton and cytoplasm were overrepresented in this data set. In addition, the biological process involved in the movement of cell or subcellular component were modified more than one would expect by chance. Previous data comparing in vivo bovine endometrium exposed to AI and cloned conceptuses has shown overrepresented processes involved in cellular transport.[5] We propose that changes to cellular transport as part of the biosensor activity of the endometrium are mediated in part via actions of miR-128 on the endometrium. In addition, the pathway of RHO GTPase cycle was also overrepresented in our in vitro data. While to our knowledge this pathway has not been previously shown to function in the bovine peri-implantation period data in other species has reported modification of members of the RHO/rock family in the luminal epithelium alters attachment of trophoblast cells,[61,62] and stromal cell function[63] in humans in vitro. While changes to members of this pathway in mouse,[64] and humans[65] can alter decidual and NK cell function. Collectively, these data suggest that these miRNAs may play a role in modifying the proteome of the endometrium to facilitate implantation in cattle and may be modified when exposed to embryos with different developmental competencies. In contrast, miR-1298 altered proteins in vitro were overrepresented in the biological processes of negative regulation of mRNA splicing and were involved in the pathways of nuclear envelope breakdown and mRNA processing suggesting these may be involved in translational control of the endometrium in response to conceptuses with different developmental competencies. Previous data from endometrium exposed to in vivo versus cloned conceptuses in cattle also identified that Transcription as a process was overrepresented in differently expressed genes in the endometria exposed to these conceptuses with different developmental competencies.[5] We propose that miR-1298 may contribute to the biosensor capability of the endometrium by modifying the translational landscape during the peri-implantation period of development.

Another key function of the endometrium is production of ULF to support the growth and development of the conceptus prior to the formation of the placenta. It is possible that differences in EV cargo are produced to signal to the endometrium to modify the composition of ULF to help tailor the specific developmental needs of the conceptus. We also provide additional evidence of the lack of robustness in terms of miRNA target prediction and that which can be demonstrated in vitro. In addition, we have determined new and novel targets of bovine miR128 and miR-1298 in a tissue-specific manner, (i.e., endometrium), demonstrating the need for further tissue and cell-specific target prediction models and in databases such as the well-curated mirGeneDB.[66]

The phenomena of the biosensor capability of the endometrium in different mammalian species with different implantation strategies have been known for over a decade.[5–7,41,67] However, the mechanism of action of how this is achieved has remained elusive. Our study clearly demonstrates that the response of the endometrium to embryos of different developmental potential (and sex) is mediated, in part, by different miRNA cargo in EVs derived from the conceptus. Specifically, we have shown that

miR-128, and miR-1298 modify the endometrial response to embryos produced using ARTs compared to in vivo-produced embryos. These data enhance our understanding of this biological phenomenon but also provide a road map for intervention to enhance developmental trajectory of the embryo and subsequent pregnancy outcome.

AUTHOR CONTRIBUTIONS

NF conceived the idea, designed and carried out the experiments, analyzed the data, and drafted the manuscript. TDB designed and conducted experiments, collected and analyzed data, and worked on the final draft of the manuscript. JCS and FVM conceived the idea, designed the experiments, and worked in the final draft of the manuscript. IGM, GAAJ, GP, RVS, AB, ACFCMA, JRS, JCBS, HT, IM-E, YFW, and AG-D performed experiments, collected data, and worked on the manuscript. RPN, DW, and EJRV analyzed and performed bioinformatics analyses. All authors approved the final version of the manuscript.

ACKNOWLEDGMENTS

We would like to acknowledge the help and assistance of students throughout the sample collection phase of this project. This work was supported by BBSRC grant number BB/R017522/1, QR-GCRF, and FAPESP (2016/22790-1, 2017/50438-3 and 2018/14137-1). We would like to acknowledge the assistance of the University of Leeds LeedsOmics facility and the University of Bristol Proteomics core facility. We acknowledge BioRender in our production of components of Figure 1 and graphical abstract. We would like to thank the staff and laboratory of flow cytometry from Hemocentro, Faculty of Medicine, University of São Paulo, Ribeirão Preto, SP, for the support in performing the cytometry analyses.

DISCLOSURES

The authors declare no competing interests.

DATA AVAILABILITY STATEMENT

The mass spectrometry proteomics data have been deposited to the ProteomeXchange Consortium via the PRIDE partner repository with the dataset identifier PXD050057. All RNA sequencing data are available via GEO database number GSE256161.

REFERENCES

1. Wiltbank MC, Baez GM, Garcia-Guerra A, et al. Pivotal periods for pregnancy loss during the first trimester of gestation in lactating dairy cows. *Theriogenology*. 2016;86:239-253.
2. Hansen TR, Sinedino LDP, Spencer TE. Paracrine and endocrine actions of interferon tau (IFNT). *Reproduction*. 2017;154:F45-F59.
3. Mamo S, Mehta JP, Forde N, McGettigan P, Lonergan P. Conceptus-endometrium crosstalk during maternal recognition of pregnancy in cattle. *Biol Reprod*. 2012;87:1-9.
4. Forde N, Bazer FW, Spencer TE, Lonergan P. 'Conceptualizing' the endometrium: identification of conceptus-derived proteins during early pregnancy in cattle. *Biol Reprod*. 2015;92:1-13.
5. Mansouri-Attia N, Sandra O, Aubert J, et al. Endometrium as an early sensor of in vitro embryo manipulation technologies. *Proc Natl Acad Sci*. 2009;106:5687-5692.
6. Bauersachs S, Ulbrich SE, Zakhartchenko V, et al. The endometrium responds differently to cloned versus fertilized embryos. *Proc Natl Acad Sci*. 2009;106:5681-5686.
7. Macklon NS, Brosens JJ. The human endometrium as a sensor of embryo quality. *Biol Reprod*. 2014;91:1-8.
8. Forde N, Lonergan P. Interferon-tau and fertility in ruminants. *Reproduction*. 2017;154:F33-F43.
9. Godkin JD, Bazer FW, Thatcher WW, Roberts RM. Proteins released by cultured day 15-16 conceptuses prolong luteal maintenance when introduced into the uterine lumen of cyclic ewes. *Reproduction*. 1984;71:57-64.
10. Thatcher WW, Bartol FF, Knickerbocker JJ, et al. Maternal recognition of pregnancy in cattle. *J Dairy Sci*. 1984;67:2797-2811.
11. Tinning H, Taylor A, Wang D, et al. The role of CAPG in molecular communication between the embryo and the uterine endometrium: is its function conserved in species with different implantation strategies? *FASEB J*. 2020;34:11015-11029.
12. Bauersachs S, Ulbrich SE, Reichenbach HD, et al. Comparison of the effects of early pregnancy with human interferon, alpha 2 (IFNA2), on gene expression in bovine endometrium. *Biol Reprod*. 2012;86:1-15.
13. Raposo G, Stoorvogel W. Extracellular vesicles: exosomes, microvesicles, and friends. *J Cell Biol*. 2013;200:373-383.
14. Desrochers LM, Bordeleau F, Reinhart-King CA, Cerione RA, Antonyak MA. Microvesicles provide a mechanism for intercellular communication by embryonic stem cells during embryo implantation. *Nat Commun*. 2016;7:11958.
15. Black SG, Arnaud F, Palmarini M, Spencer TE. Endogenous retroviruses in trophoblast differentiation and placental development. *Am J Reprod Immunol*. 2010;64:255-264.
16. Burns G, Brooks K, Wildung M, Navakanitworakul R, Christenson LK, Spencer TE. Extracellular vesicles in luminal fluid of the ovine uterus. *PLoS One*. 2014;9:e90913.
17. Machtinger R, Laurent LC, Baccarelli AA. Extracellular vesicles: roles in gamete maturation, fertilization and embryo implantation. *Hum Reprod Update*. 2015;22:182-193.
18. Kropp J, Salih SM, Khatib H. Expression of microRNAs in bovine and human pre-implantation embryo culture media. *Front Genet*. 2014;5:91.
19. Rosenbluth EM, Shelton DN, Wells LM, Sparks AET, van Voorhis BJ. Human embryos secrete microRNAs into culture media—a potential biomarker for implantation. *Fertil Steril*. 2014;101:1493-1500.
20. Bridi A, Andrade GM, del Collado M, et al. Small extracellular vesicles derived from in vivo- or in vitro-produced bovine blastocysts have different miRNAs profiles—implications for embryo-maternal recognition. *Mol Reprod Dev*. 2021;88:628-643.
21. Parrish JJ, Susko-Parrish J, Winer MA, First NL. Capacitation of bovine sperm by heparin. *Biol Reprod*. 1988;38:1171-1180.

22. De Bem THC, Da Silveira JC, Sampaio RV, et al. Low levels of exosomal-miRNAs in maternal blood are associated with early pregnancy loss in cloned cattle. *Sci Rep*. 2017;7:14319.
23. De Bem THC, Chiaratti MR, Rochetti R, et al. Viable calves produced by somatic cell nuclear transfer using meiotic-blocked oocytes. *Cell Reprogram*. 2011;13:419-429.
24. De Bem THC, Adona P, Bressan F, et al. The influence of morphology, follicle size and Bcl-2 and Bax transcripts on the developmental competence of bovine oocytes. *Reprod Domest Anim*. 2014;49:576-583.
25. Crescitelli R, Lässer C, Szabó TG, et al. Distinct RNA profiles in subpopulations of extracellular vesicles: apoptotic bodies, microvesicles and exosomes. *J Extracell Vesicles*. 2013;2:20677.
26. Martin M. Cutadapt removes adapter sequences from high-throughput sequencing reads. *EMBnet J*. 2011;17:10-12.
27. Langmead B, Trapnell C, Pop M, Salzberg SL. Ultrafast and memory-efficient alignment of short DNA sequences to the human genome. *Genome Biol*. 2009;10:1-10.
28. Kitts PA, Church DM, Thibaud-Nissen F, et al. Assembly: a resource for assembled genomes at NCBI. *Nucleic Acids Res*. 2016;44:D73-D80.
29. Li H, Handsaker B, Wysoker A, et al. The sequence alignment/map format and SAMtools. *Bioinformatics*. 2009;25:2078-2079.
30. Liao Y, Smyth GK, Shi W. featureCounts: an efficient general purpose program for assigning sequence reads to genomic features. *Bioinformatics*. 2014;30:923-930.
31. Kozomara A, Birgaoanu M, Griffiths-Jones S. miRBase: from microRNA sequences to function. *Nucleic Acids Res*. 2019;47:D155-D162.
32. Love MI, Huber W, Anders S. Moderated estimation of fold change and dispersion for RNA-seq data with DESeq2. *Genome Biol*. 2014;15:1-21.
33. Dobin A, Davis CA, Schlesinger F, et al. STAR: ultrafast universal RNA-seq aligner. *Bioinformatics*. 2013;29:15-21.
34. Liao Y, Smyth GK, Shi W. The R package Rsubread is easier, faster, cheaper and better for alignment and quantification of RNA sequencing reads. *Nucleic Acids Res*. 2019;47:e47.
35. Robinson MD, McCarthy DJ, Smyth GK. edgeR: a Bioconductor package for differential expression analysis of digital gene expression data. *Bioinformatics*. 2010;26:139-140.
36. Yu G, Wang LG, Han Y, He QY. clusterProfiler: an R package for comparing biological themes among gene clusters. *OMICS*. 2012;16:284-287.
37. Luo W, Brouwer C. Pathview: an R/Bioconductor package for pathway-based data integration and visualization. *Bioinformatics*. 2013;29:1830-1831.
38. Wickham H. *ggplot2*. Springer International Publishing; 2016.
39. Kolde R. pheatmap: Pretty Heatmaps. *R Packag*. 2019.
40. Hume L, Edge JC, Tinning H, et al. MicroRNAs emerging coordinate with placental mammals alter pathways in endometrial epithelia important for endometrial function. *iScience*. 2023;26:106339.
41. Sandra O, Constant F, Vitorino CA, et al. Maternal organism and embryo biosensoring: insights from ruminants. *J Reprod Immunol*. 2015;108:105-113.
42. Tinning H, Edge JC, De Bem THC, et al. Review: endometrial function in pregnancy establishment in cattle. *Animal*. 2023;17:100751.
43. Forde N, Carter F, Fair T, et al. Progesterone-regulated changes in endometrial gene expression contribute to advanced conceptus development in cattle. *Biol Reprod*. 2009;81:784-794.
44. Forde N, Mehta JP, Minten M, et al. Effects of low progesterone on the endometrial transcriptome in cattle. *Biol Reprod*. 2012;87:1-11.
45. Forde N, Beltman ME, Duffy GB, et al. Changes in the endometrial transcriptome during the bovine estrous cycle: effect of low circulating progesterone and consequences for conceptus elongation. *Biol Reprod*. 2011;84:266-278.
46. Forde N, Mehta JP, McGettigan PA, et al. Alterations in expression of endometrial genes coding for proteins secreted into the uterine lumen during conceptus elongation in cattle. *BMC Genomics*. 2013;14:1-13.
47. Théry C, Witwer KW, Aikawa E, et al. Minimal information for studies of extracellular vesicles 2018 (MISEV2018): a position statement of the International Society for Extracellular Vesicles and update of the MISEV2014 guidelines. *J Extracell Vesicles*. 2018;7:1535750.
48. Chaney HL, Grose LF, LaBarbara JM, et al. Galectin-1 induces gene and protein expression related to maternal-conceptus immune tolerance in bovine endometrium. *Biol Reprod*. 2022;106:487-502.
49. O'Neil EV, Burns GW, Spencer TE. Extracellular vesicles: novel regulators of conceptus-uterine interactions? *Theriogenology*. 2020;150:106-112.
50. Nakamura K, Kusama K, Ideta A, Imakawa K, Hori M. IFNT-independent effects of intrauterine extracellular vesicles (EVs) in cattle. *Reproduction*. 2020;159:503-511.
51. Nakamira K, Kusama K, Hori M, et al. Global analyses and potential effects of extracellular vesicles on the establishment of conceptus implantation during the peri-implantation period. *J Reprod Dev*. 2023;69:2023-2044.
52. Guzewska MM, Myszczynski K, Heifetz Y, Kaczmarek MM. Embryonic signals mediate extracellular vesicle biogenesis and trafficking at the embryo–maternal interface. *Cell Commun Signal*. 2023;21:210.
53. Guzewska MM, Witek KJ, Karnas E, et al. miR-125b-5p impacts extracellular vesicle biogenesis, trafficking, and EV subpopulation release in the porcine trophoblast by regulating ESCRT-dependent pathway. *FASEB J*. 2023;37:e23054.
54. Burns GW, Brooks KE, Spencer TE. Extracellular vesicles originate from the conceptus and uterus during early pregnancy in sheep. *Biol Reprod*. 2016;94:56-61.
55. Ruiz-González I, Minten M, Wang X, Dunlap KA, Bazer FW. Involvement of TLR7 and TLR8 in conceptus development and establishment of pregnancy in sheep. *Reproduction*. 2015;149:305-316.
56. Hamdi M, Cañon-Beltrán K, Mazzarella R, et al. Characterization and profiling analysis of bovine oviduct and uterine extracellular vesicles and their miRNA cargo through the estrous cycle. *FASEB J*. 2021;35:e22000.
57. Forde N, Maillo V, O'Gaora P, et al. Sexually dimorphic gene expression in bovine conceptuses at the initiation of implantation. *Biol Reprod*. 2016;95:92-101.
58. Bazer FW, Burghardt RC, Johnson GA, Spencer TE, Wu G. Mechanisms for the establishment and maintenance of pregnancy: synergies from scientific collaborations. *Biol Reprod*. 2018;99:225-241.

59. Bermejo-Alvarez P, Ramos-Ibeas P, Gutierrez-Adan A. Solving the "X" in embryos and stem cells. *Stem Cells Dev*. 2012;21:1215-1224.
60. Hansen PJ, Dobbs KB, Denicol AC, Siqueira LGB. Sex and the preimplantation embryo: implications of sexual dimorphism in the preimplantation period for maternal programming of embryonic development. *Cell Tissue Res*. 2016;363:237-247.
61. Heneweer C. Adhesiveness of human uterine epithelial RL95-2 cells to trophoblast: rho protein regulation. *Mol Hum Reprod*. 2002;8:1014-1022.
62. Garrido-Gómez T, Dominguez F, Quiñonero A, et al. Annexin A2 is critical for embryo adhesiveness to the human endometrium by RhoA activation through F-Actin regulation. *FASEB J*. 2012;26:3715-3727.
63. Grewal S, Carver J, Ridley AJ, Mardon HJ. Human endometrial stromal cell rho GTPases have opposing roles in regulating focal adhesion turnover and embryo invasion in Vitro1. *Biol Reprod*. 2010;83:75-82.
64. Davila J, Laws MJ, Kannan A, et al. Rac1 regulates endometrial secretory function to control placental development. *PLoS Genet*. 2015;11:e1005458.
65. Zhang D, Yu Y, Ding C, Zhang R, Duan T, Zhou Q. Decreased B7-H3 promotes unexplained recurrent miscarriage via RhoA/ROCK2 signaling pathway and regulates the secretion of decidual NK cells. *Biol Reprod*. 2023;108:504-518.
66. Fromm B, Høye E, Domanska D, et al. MirGeneDB 2.1: toward a complete sampling of all major animal phyla. *Nucleic Acids Res*. 2022;50:D204-D210.
67. Bazer FW, Song G, Kim J, et al. Uterine biology in pigs and sheep. *J Anim Sci Biotechnol*. 2012;3:1-21.

SUPPORTING INFORMATION

Additional supporting information can be found online in the Supporting Information section at the end of this article.

How to cite this article: De Bem THC, Bridi A, Tinning H, et al. Biosensor capability of the endometrium is mediated in part, by altered miRNA cargo from conceptus-derived extracellular vesicles. *The FASEB Journal*. 2024;38:e23639. doi:10.1096/fj.202302423RR